
Princeton Plasma Physics Laboratory

PPPL-

PPPL-



Prepared for the U.S. Department of Energy under Contract DE-AC02-09CH11466.

Princeton Plasma Physics Laboratory

Report Disclaimers

Full Legal Disclaimer

This report was prepared as an account of work sponsored by an agency of the United States Government. Neither the United States Government nor any agency thereof, nor any of their employees, nor any of their contractors, subcontractors or their employees, makes any warranty, express or implied, or assumes any legal liability or responsibility for the accuracy, completeness, or any third party's use or the results of such use of any information, apparatus, product, or process disclosed, or represents that its use would not infringe privately owned rights. Reference herein to any specific commercial product, process, or service by trade name, trademark, manufacturer, or otherwise, does not necessarily constitute or imply its endorsement, recommendation, or favoring by the United States Government or any agency thereof or its contractors or subcontractors. The views and opinions of authors expressed herein do not necessarily state or reflect those of the United States Government or any agency thereof.

Trademark Disclaimer

Reference herein to any specific commercial product, process, or service by trade name, trademark, manufacturer, or otherwise, does not necessarily constitute or imply its endorsement, recommendation, or favoring by the United States Government or any agency thereof or its contractors or subcontractors.

PPPL Report Availability

Princeton Plasma Physics Laboratory:

<http://www.pppl.gov/techreports.cfm>

Office of Scientific and Technical Information (OSTI):

<http://www.osti.gov/bridge>

Related Links:

[U.S. Department of Energy](#)

[Office of Scientific and Technical Information](#)

[Fusion Links](#)

Contained modes in mirrors with sheared rotation

Abraham J. Fetterman and Nathaniel J. Fisch

Department of Astrophysical Sciences, Princeton University, Princeton, New Jersey 08540, USA

(Dated: 14 October 2010)

In mirrors with $E \times B$ rotation, a fixed azimuthal perturbation in the lab frame can appear as a wave in the rotating frame. If the rotation frequency varies with radius, the plasma-frame wave frequency will also vary radially due to the Doppler shift. A wave that propagates in the high rotation plasma region might therefore be evanescent at the plasma edge. This can lead to radially localized Alfvén eigenmodes with high azimuthal mode numbers. Contained Alfvén modes are found both for peaked and non-peaked rotation profiles. These modes might be useful for alpha channeling or ion heating, as the high azimuthal wave number allows the plasma wave frequency in the rotating frame to exceed the ion cyclotron frequency.

I. INTRODUCTION

Rotating mirrors exhibit the simplicity, high beta, and steady state operation of axisymmetric mirrors as well as enhanced confinement and stability due to supersonic rotation.^{1,2} For these reasons, mirrors with centrifugal confinement have been proposed as attractive fusion reactors.³⁻⁵ A major impediment to progress on these devices is the Alfvén critical ionization velocity (CIV) limitation. The Alfvén CIV limitation occurs at the interface between the moving plasma and stationary electrode or insulator.^{1,6,7} It has been suggested that the CIV limit could be overcome by driving a radial current to produce rotation using waves rather than end electrodes.⁸⁻¹¹

The method for driving rotation with waves is an extension of the alpha channeling effect in tokamaks and stationary mirrors.¹²⁻¹⁵ In alpha channeling, radio frequency waves are used to create diffusion paths for alpha particles from the hot center of the plasma to the cold edge. The energy lost by the alpha particle in exiting the plasma is transferred to the wave. In rotating plasmas, when the alpha particles interact with the wave and diffuse outward, they increase their potential energy at the expense of kinetic energy, effectively creating a radial current that drives rotation.⁸

The branching ratio f_E was used to describe the wave-particle interaction in rotating plasmas. The branching ratio is the ratio of the increase in potential energy to the decrease in kinetic energy of a particle, which in a slab geometry is $f_E = v_E / (v_E - v_{ph})$, where $v_E = E/B$ is the drift velocity and $v_{ph} = \omega/k$ is the phase velocity. One can see that a fixed ripple in the lab frame, with $v_{ph} = 0$, will have $f_E = 1$, so no energy is transferred to or from the wave.¹⁰ This is a simple, passive way to drive rotation and utilize alpha particle energy, in addition to removing the fusion ash. One challenge is that high mode-number waves are required to satisfy the alpha particle cyclotron resonance condition, $m \approx -\Omega_i / \Omega \gtrsim 20$, where Ω is the rotation frequency and Ω_i is the cyclotron frequency. These modes are mostly evanescent in the plasma.

Although these waves are evanescent near the antenna, it turns out that they may be excited efficiently as internal modes, much like in tokamaks. In the tokamak geom-

etry, contained Alfvén modes exist that are destabilized by alpha particles and are responsible for turbulence in the ion cyclotron range of frequencies.¹⁶ These modes may be useful in alpha channeling in tokamaks, where there are advantages to using low frequency waves, like the ion Bernstein wave,^{14,17} although for somewhat different reasons than in mirror machines.¹⁸

However, when ion Bernstein waves were excited in the Tokamak Fusion Test Reactor (TFTR) to test alpha channeling, the surprising result was diffusion rates fifty times higher than those predicted by quasilinear theory.^{19,20} Although it seemed implausible, the only explanation for such a dramatic increase in diffusion was that a toroidal cavity mode was excited. The existence of such high-Q cavity modes was later shown to in fact be quite plausible,²¹ and has recently been supported by measurements on the National Spherical Torus Experiment.²² If the very large diffusion achieved by these modes can also be accomplished in a tokamak reactor, then the reactor costs would be significantly reduced.

What most interests us here is that there has been considerable experimental and theoretical support for these kinds of modes and the effects they can play in alpha channeling in similar geometries. This lends support to the proposals outlined in this paper, where we describe a similar contained mode for plasmas with sheared rotation. Consider a low frequency wave that is evanescent outside the plasma. Inside the rotating plasma, this wave may appear at a higher frequency due to the Doppler shift. As the rotating frame frequency increases, the evanescent wave may go through a cutoff and become a propagating wave. As it propagates inward, it will reach another cutoff, either due to convergence (since k_θ^2 increases as the radius decreases) or due to a decreasing rotation frequency (for example if there is an inner wall). The Alfvén wave is reflected at these cutoffs, so the energy is contained and high amplitudes can be achieved.

Rotation shear has been found to stabilize high mode number, low frequency modes in mirror plasmas.²³⁻²⁵ It is therefore unusual that sheared rotation should lead to waves with high mode numbers. However, in this case higher mode numbers have higher frequencies in the plasma frame, and we will show that they are not effec-

tively damped by the velocity shear.

Because the modes can have high azimuthal mode numbers and zero frequency in the lab frame, they may couple to the fixed ripple used for alpha channeling. This would increase the alpha channeling efficiency by increasing the wave amplitude in the peak rotation region where most alpha particles are produced. This mode may also provide an efficient method of plasma heating if the rotating frame frequency coincides with a cyclotron harmonic.

Because the wave phase velocity is near the Alfvén velocity, we expect zero frequency contained modes to exist only if the rotation speed is near the Alfvén speed. Recent experiments on MCX have suggested that the Alfvén mach number cannot exceed unity.^{30,31} These experiments observe a limit on the average Alfvén mach number defined by $\bar{M}_A = V_p/aB\bar{v}_A$, where V_p is the voltage across the plasma, a is the plasma width, and \bar{v}_A is the Alfvén velocity based on a line-averaged density. The theory supporting the Alfvén mach number limit requires a cylindrical plasma with uniform rotation. Because the rotation profile is nonuniform, there is no conflict with the requirement that the peak Alfvén mach number $M_A > 1$. In fact for values of \bar{M}_A near unity it is very likely that $M_A > 1$. We therefore think that the modes described here are of interest in MCX and other supersonically rotating plasmas.

This paper will be organized as follows. In Section II, we will derive the eigenmode equation for the contained modes. We will then in Section III find the properties of contained modes assuming a peaked rotation profile. Mode properties for plasmas without a strong peak will be addressed in Section IV. We will then discuss ion cyclotron absorption of these modes in Section V. Our conclusions will be presented in Section VI.

II. EIGENMODE EQUATION

The contained modes are localized eigenmode solutions to the MHD equations,

$$\rho \left(\frac{\partial}{\partial t} + \mathbf{v} \cdot \nabla \right) \mathbf{v} = \frac{1}{c} \mathbf{J} \times \mathbf{B}, \quad (1)$$

$$0 = \mathbf{E} + \frac{1}{c} \mathbf{v} \times \mathbf{B} - \frac{1}{cne} \mathbf{J} \times \mathbf{B}. \quad (2)$$

The first of these is the force balance equation, and the second is Ohm's law. We will assume the equilibrium is $\mathbf{B}_0 = B_0 \hat{z}$, $\mathbf{J}_0 = 0$, $\mathbf{v}_0 = r\Omega(r)\hat{\theta}$, and $\mathbf{E}_0 = -r\Omega(r)B_0\hat{r}/c$. We have defined $\Omega(r)$ as the rotation frequency at radius r . This equilibrium neglects the diamagnetic effect of the centrifugal force. Because we will find localized solutions, this is a good approximation even for finite beta plasmas.

We seek solutions proportional to $\exp(im\theta + ik_{\parallel}z - i\omega t)$. The linearization of the second term on the left of Eq. (1) is, to first order,

$$\mathbf{v} \cdot \nabla \mathbf{v} = \Omega im \mathbf{v}_1 - 2v_{1\theta} \Omega \hat{r} + 2\Omega v_{1r} \hat{\theta} + v_{1r} r \Omega' \hat{\theta}. \quad (3)$$

Here we have omitted the dependence of Ω on r and use primes to denote radial derivatives. The terms on the right of Eq. (3) represent the Doppler, centrifugal, Coriolis, and convection terms respectively. We will neglect the centrifugal and Coriolis effects, which are much smaller than the Doppler term assuming $m \gg 2$. The linearized form of Eq. (1) is then,

$$\rho(-i\omega + \Omega im) \mathbf{v}_1 = \frac{1}{c} \mathbf{J}_1 \times \mathbf{B}_0 - \rho v_{1r} r \Omega' \hat{\theta}. \quad (4)$$

When we take the curl of Eq. (2), apply Faraday's law and linearize, we find,

$$-i\omega \mathbf{B}_1 = \nabla \times \left[\mathbf{v}_1 \times \mathbf{B}_0 + \mathbf{v}_0 \times \mathbf{B}_1 - \frac{1}{ne} \mathbf{J}_1 \times \mathbf{B}_0 \right]. \quad (5)$$

We finally get a single differential equation for \mathbf{B}_1 by substituting Ampere's law, $\mathbf{J}_1 = \frac{c}{4\pi} \nabla \times \mathbf{B}_1$, and the velocity from Eq. (4) into Eq. (5). We define the plasma-frame frequency as $\tilde{\omega} = \omega - m\Omega$, and find,

$$\begin{aligned} -i\omega \mathbf{B}_1 = \nabla \times & \left[\left(i \frac{1}{4\pi\rho\tilde{\omega}} (\nabla \times \mathbf{B}_1) \times \mathbf{B}_0 \right) \times \mathbf{B}_0 \right. \\ & - i \frac{v_{1r}r}{\tilde{\omega}} \Omega' \hat{\theta} \times \mathbf{B}_0 + \mathbf{v}_0 \times \mathbf{B}_1 \\ & \left. - \frac{c}{4\pi ne} (\nabla \times \mathbf{B}_1) \times \mathbf{B}_0 \right]. \end{aligned} \quad (6)$$

Using this equation, one can find expressions for B_{1r} and $B_{1\theta}$ in terms of B_{1z} and its derivative. A differential equation for B_{1z} can then be obtained. These calculations are performed in the Appendix.

A rough approximation of the result may be found by considering a plasma with solid body rotation ($\Omega' = 0$) and waves with $k_{\parallel} = 0$. In this case, we recover the equation from Coppi,¹⁶ with the substitution of the rotating frame frequency,

$$\frac{1}{r} \frac{d}{dr} \left(r \frac{dB_{1z}}{dr} \right) + \left[\frac{\tilde{\omega}^2}{v_A^2} - k_{\theta}^2 \right] B_{1z} = 0.$$

If we scale B_{1z} to $b_1 = B_{1z}\sqrt{r}$, we can write this in terms of an effective potential V_{eff} ,

$$\frac{d^2 b_1}{dr^2} - V_{\text{eff}}(r, \omega) b_1 = 0; \quad V_{\text{eff}} = k_{\theta}^2 - \frac{\tilde{\omega}^2}{v_A^2}. \quad (7)$$

The first term in the above effective potential varies with a scale length of the device radius, since $k_{\theta}^2 = m^2/r^2$. For solid body rotation, the second term is constant, but with sheared rotation the plasma frame frequency $\tilde{\omega} = \omega - m\Omega(r)$ can vary rapidly over the plasma width. If the potential has a minimum below zero, there can be a localized solution to the oscillator equation. Because the plasma width is much smaller than the device radius, the second term will be dominant in determining the location of the potential minimum. For the solution to be bounded we must also have $V_{\text{eff}} > 0$ in a region inside and outside the local minimum.

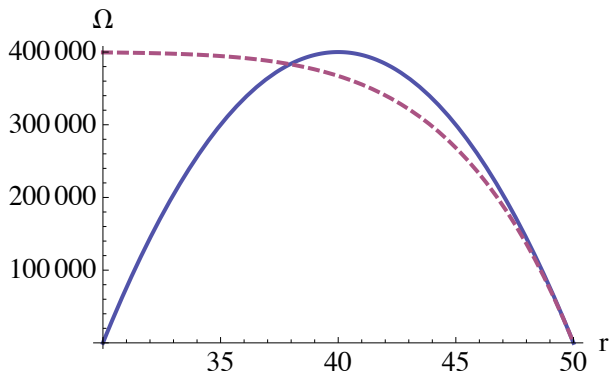


FIG. 1. Rotation frequency (s^{-1}) versus radius (in cm) for the peaked case (solid) and non-peaked (dashed).

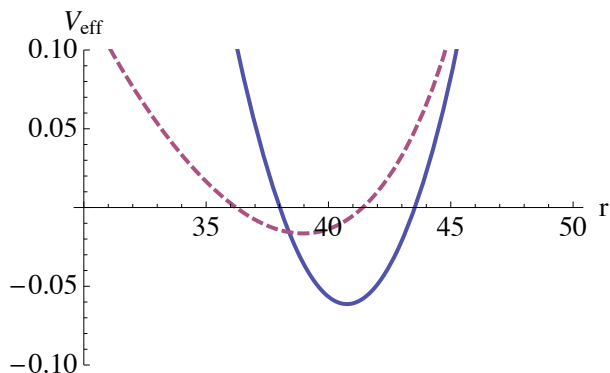


FIG. 2. Example effective potential (cm^{-2}) versus radius (in cm) for the peaked case (solid) and non-peaked (dashed). The mode parameters are $m = -20$, $\omega = 0$, and $M_A = 1.2$.

In many rotating plasma experiments, there is supersonic rotation in the middle of the plasma region, but at walls near the axis of rotation and outside the plasma, the rotation goes to zero (Fig. 1, solid line).^{1,26,27} In these devices, low frequency waves with high azimuthal mode number will produce a minimum in V_{eff} near where the peak rotation frequency Ω_0 occurs, at radius r_{Ω_0} (see Fig. 2). If $V_{\text{eff}}(r_{\Omega_0}, \omega) < 0$, then a contained mode may exist near r_{Ω_0} .

Because we expect the modes to be approximately perpendicular, we will continue to assume that $k_{\parallel} = 0$. In addition, we will assume that the rotation scale length $d \ll r$, and that $\Omega \ll \Omega_i$, the ion cyclotron frequency. When we apply these assumptions, we find that the effective potential for rotating plasmas with shear is,

$$V_{\text{eff}} \approx \left(1 + \frac{\Omega}{\Omega_i}\right) k_{\theta}^2 - \frac{\tilde{\omega}^2}{v_A^2} + 2 \frac{m\Omega'}{\tilde{\omega}r} + 2 \frac{m^2\Omega'^2}{\tilde{\omega}^2} + \frac{m\Omega''}{\tilde{\omega}}. \quad (8)$$

Because the mode is localized near the radius of peak rotation, we will find that the Ω' terms do not contribute significantly to the first order mode behavior.

III. CONTAINED MODE

To find a localized solution, we can treat the potential V_{eff} as parabolic by expanding around its minimum r_m . For this expansion we adopt the ordering $k_{\theta}^2 \gg 1/\Delta^2 \gg 1/r^2$, valid for $m^2 \gg 1$, where Δ is the width of the localized mode $b(r)$. A solution to the differential equation is then,

$$b(r) = bH_s \left(\frac{r - r_m}{\Delta} \right) \exp \left(-\frac{(r - r_m)^2}{2\Delta^2} \right). \quad (9)$$

Here H_s is the Hermite polynomial of order s , s is a positive integer, r_m is the mode radius and Δ is the mode width. The width, radius and frequency must satisfy the relationships,

$$V_{\text{eff}}(r_m, \omega) = -\frac{2s+1}{\Delta^2}, \quad (10)$$

$$\frac{dV_{\text{eff}}(r_m, \omega)}{dr} = 0, \quad (11)$$

$$\frac{d^2V_{\text{eff}}(r_m, \omega)}{dr^2} = \frac{2}{\Delta^4}. \quad (12)$$

We will assume that the rotation frequency is peaked at some value Ω_0 at radius r_{Ω_0} , and that the $\tilde{\omega}^2$ term in Eq. (8) dominates the radial variation. We then use radius r_{Ω_0} as an approximate value for r_m , the location of the potential minimum.

In order to estimate V_{eff} near r_{Ω_0} , we expand $\Omega(r)$ as a series around r_{Ω_0} using $r = r_{\Omega_0} + r_1$, and define the rotation scale length d through $\Omega(r) = \Omega_0 (1 - r_1^2/d^2)$. Then defining $M_A = \Omega_0 r_{\Omega_0}/v_A$, $k_{\theta} = m/r_{\Omega_0}$, and $\epsilon = \omega/m\Omega_0$,

$$V_{\text{eff}}'' \approx \frac{4}{d^4} \left(k_{\theta}^2 d^2 M_A^2 (1 - \epsilon) + \frac{3}{(1 - \epsilon)^2} \right). \quad (13)$$

The approximation uses the assumptions $d^2 \ll r_{\Omega_0}^2$ and $\chi = \Omega_0/\Omega_i \ll 1$. Using Eqs. (12) and (13), we find that the mode width $\Delta \approx d / (2k_{\theta}^2 d^2 M_A^2 + 6)^{1/4}$ for small ϵ . For this result to be consistent with the ordering $k_{\theta}^2 \gg 1/\Delta^2$, we consider mode numbers $k_{\theta}^2 d^2 \gg 3$. Using this assumption along with $\epsilon \ll 1$ we may further simplify Eq. (13),

$$V_{\text{eff}}'' \approx \frac{4k_{\theta}^2 M_A^2}{d^2}. \quad (14)$$

This result may also be obtained directly from the simplified form for the potential, Eq. (7).

We can now use Eq. (11) to find the distance of the mode from the radius of peak rotation $\delta r = r_m - r_{\Omega_0}$,

$$0 = -2(1 + \chi) \frac{m^2}{r_{\Omega_0}^3} + V_{\text{eff}}'' \delta r. \quad (15)$$

Substituting in Eq. (13),

$$\delta r = \frac{k_{\theta}^2 d^4 (1 - \epsilon)^2 (1 + \chi)}{2r_{\Omega_0} (k_{\theta}^2 d^2 M_A^2 (1 - \epsilon)^3 + 3)}. \quad (16)$$

Because $\delta r \approx d^2/2r_{\Omega 0}$ is small compared to d , we have verified that the mode location is near the radius of peak rotation.

We finally will find the potential at r_m , which will allow us to determine the normalized frequency $\epsilon = \omega/m\Omega_0$ of the mode using Eq. (10). To simplify the expression, we note that at r_m , $V'_{\text{eff}}(r_m) = 0$ and $\frac{1}{2}V''_{\text{eff}}\delta r^2/k_\theta^2 \lesssim d^2/r_{\Omega 0}^2 \ll 1$. Therefore, the potential $V_{\text{eff}}(r_m) \approx V_{\text{eff}}(r_{\Omega 0})$,

$$V_{\text{eff}}(r_m) \approx k_\theta^2 - (1 - \epsilon)^2 k_\theta^2 M_A^2 + \frac{2}{(1 - \epsilon)d^2}. \quad (17)$$

This equation may be combined with Eqs. (10), (12) and (13), defining $\alpha = (2s + 1)$. The result is,

$$0 = 1 - (1 - \epsilon)^2 M_A^2 + \frac{2}{(1 - \epsilon)k_\theta^2 d^2} + \frac{\sqrt{2}\alpha}{k_\theta^2 d^2} \left(k_\theta^2 d^2 M_A^2 (1 - \epsilon) + \frac{3}{(1 - \epsilon)^2} \right)^{1/2}. \quad (18)$$

We use our previous orderings together with $\epsilon \ll 1$, and find to first order

$$\epsilon \approx \frac{M_A^2 - 1 - \sqrt{2}\alpha M_A / |k_\theta d|}{2M_A^2 - \alpha M_A / |k_\theta d| \sqrt{2}}. \quad (19)$$

We can now find the rotation speed necessary for contained modes to be resonant with a stationary perturbation ($\epsilon = 0$), assuming $|k_\theta d| \ll \alpha$,

$$M_A \approx 1 + \frac{\alpha/\sqrt{2}}{|k_\theta d|}. \quad (20)$$

This implies that the Alfvén mach number needs to be just above unity. Accurate values for the rotation speed at which $\epsilon = 0$ should be obtained by solving Eq. (18) directly. For very large values of $k_\theta d$, the χ and δr^2 terms will be relevant in Eq. (17) and therefore should be included in the calculation.

We finally want to know how finite values of k_\parallel will effect our results. Assuming $k_\parallel^2 \ll \tilde{\omega}^2/v_A^2$, we may re-derive the potential V_{eff} using the equations in the Appendix. We find that the largest contribution is from an additional term equal to $k_\parallel^2 (1 + \tilde{\omega}^2/\Omega_i^2)$. The second derivative of this term is,

$$\delta V''_{\text{eff}} = -\frac{4}{d^4} k_\theta^2 d^2 k_\parallel^2 r_{\Omega 0}^2 \chi^2 (1 - \epsilon). \quad (21)$$

Comparing this to the first term in Eq. (13), we find that the k_\parallel^2 contribution to V''_{eff} is small if $k_\parallel^2 r_{\Omega 0}^2 \chi^2 \ll 1$.

Finite values of k_\parallel^2 enter Eq. (18) for the frequency both through the added term proportional to k_\parallel^2 and through the contribution of that term to V''_{eff} . These terms have opposite signs, and so the resulting change in frequency (and therefore necessary rotation speed) may be either positive or negative.

IV. MONOTONIC ROTATION PROFILE

In plasmas with sheared rotation, it may be desirable to have a monotonic rotation profile so that the region without shear is minimized (see Fig. 1, dashed line). In this case there can still be contained modes, as the radial mode number k_r goes through a cutoff because of increasing $k_\theta^2 = m^2/r^2$ at smaller radii. Because rotation shear and the second derivative of the rotation frequency are smaller near the mode, we will apply the simplified potential of Eq. (7).

We will not choose a specific rotation profile in this case, but will assume that there is some radius r_0 where the rotation frequency is Ω_0 , at which Eq. (11) is satisfied,

$$0 = -2\frac{m^2}{r_0^3} + \frac{2(\omega - m\Omega_0)m\Omega'}{v_A^2}. \quad (22)$$

The result is $\Omega'(r_0) = -\Omega_0(1 - \epsilon)/M_A^2 r_0$, where $M_A = \Omega_0 r_0/v_A$. We will assume that this slope is changing over length scale $d/2$, so $\Omega''(r_0) = 2\Omega'(r_0)/d$, and that $d \ll r_0$. With this assumption, we find the second derivative of the potential,

$$V''_{\text{eff}} \approx 4(1 - \epsilon) \frac{k_\theta^2}{r_0 d}, \quad (23)$$

where $k_\theta = m/r_0$. Therefore the width $\Delta \approx (r_0 d/2k_\theta^2)^{1/4}$, which is slightly wider than the width for the peaked rotation profile, because the mode is not in such a steep potential well (see Fig. 2).

Now using Eq. (10),

$$0 = k_\theta^2 - (1 - \epsilon)^2 k_\theta^2 M_A^2 + \alpha \sqrt{(1 - \epsilon)^2 \frac{2k_\theta^2}{r_0 d}}. \quad (24)$$

Assuming ϵ is small, we find,

$$\epsilon = \frac{M_A^2 - 1 - \sqrt{2}\alpha/\sqrt{k_\theta^2 r_0 d}}{2M_A^2 - \sqrt{2}\alpha/\sqrt{k_\theta^2 r_0 d}}. \quad (25)$$

The Alfvén mach number for fixed waves to be resonant with contained modes is then $M_A = 1 + \sqrt{2}\alpha/\sqrt{k_\theta^2 r_0 d}$. This is also just above unity, but is different from the requirement for the peaked rotation case.

V. CYCLOTRON DAMPING

A possible application for the contained modes is ion heating. The rotating frame frequency of an azimuthal magnetic ripple may be tuned to a high ion cyclotron harmonic, or to a minority ion cyclotron frequency. No wave power is absorbed because the wave has no energy in the rest frame. The dissipated power is provided through the radial electric field, which does not suffer from the coupling inefficiency of radio frequency waves. Ion heating

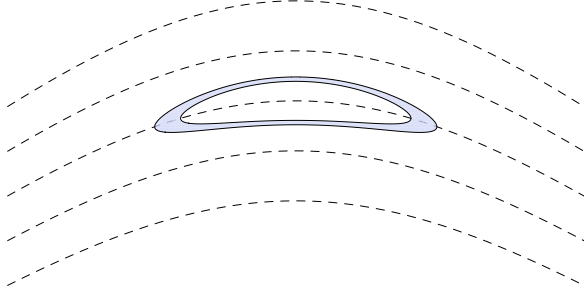


FIG. 3. A cross section of the plasma region near the midplane. The shaded region indicates the location of resonant absorption. Dashed lines indicate magnetic field lines, and the center line is at the peak rotation frequency. Here $-m\Omega_0/\Omega_{s0} = 1.05$ and $k_{\parallel}v_{th}/\Omega_{s0} = 0.01$.

may improve the flexibility of rotating plasmas by allowing control of the ion temperature independently from the rotation speed.

The power dissipated due to the wave must be provided by the radial electric field if the wave is stationary.

$$\int dV n_{res} \approx n |k_{\parallel}| \int dV \delta \left[\Omega_{i0} + \Omega_{s0} \frac{z^2}{L_z^2} + m\Omega_0 - m\Omega_0 \frac{(r - r_{\Omega_0}(z))^2}{d^2} \right]. \quad (28)$$

We integrate this result over z neglecting the z dependence of r_{Ω_0} ,

$$\int dV n_{res} \approx n \int 2\pi r dr \frac{|k_{\parallel}| L_z}{\sqrt{\left[m\Omega_0 \frac{(r - r_{\Omega_0})^2}{d^2} - \Omega_{s0} - m\Omega_0 \right] \Omega_{s0}}}. \quad (29)$$

Doing the r integration, assuming $d \ll r_{\Omega_0}$,

$$\int dV n_{res} \approx n 2\pi^2 r_{\Omega_0} d \frac{|k_{\parallel}| L_z}{\sqrt{-m\Omega_0 \Omega_{s0}}}. \quad (30)$$

The resulting absorbed power is, if we assume the electric field is uniform over the resonance region,

$$P_{\perp} = \frac{\omega_{ps}^2}{4} |E^+|^2 \frac{2\pi^2 r_{\Omega_0} L_z d}{\sqrt{-m\Omega_0 \Omega_{s0}}}. \quad (31)$$

For cyclotron heating of the primary species, it is necessary to use a high harmonic of the cyclotron frequency because the polarization of the wave becomes right-handed at the fundamental.²⁹ For stationary waves, this requires azimuthal mode number $m = n\chi^{-1} \geq 40$. Exciting such a high mode number may not be feasible. Instead, we suggest using minority heating at the fundamental. Using a heavier minority species, such as deuterium (for a hydrogen plasma), will further reduce the necessary mode number because χ is increased.

However, the power can be calculated as wave damping in the rotating frame in the same way as ICRF heating.²⁸ The absorbed power is therefore,

$$P_{\perp} = \frac{\pi Z_s^2 e^2}{m_s |k_{\parallel}|} |E^+|^2 n_{res}(\mathbf{r}, v_{\parallel}). \quad (26)$$

The number of resonant particles is, after integrating over the perpendicular directions,

$$n_{res} \approx n \int dv_{\parallel} \frac{e^{-v_{\parallel}^2/2v_{th}^2}}{\sqrt{2\pi}v_{th}} \delta \left(v_{\parallel} + \frac{\Omega_s + m\Omega_0}{k_{\parallel}} \right). \quad (27)$$

Assuming $k_{\parallel}v_{th} \ll \Omega_s + m\Omega_0$, the exponential term is approximately $\delta(v_{\parallel})$. Doing the v_{\parallel} integral, we integrate over space, adopting a peaked profile for Ω and using $\Omega_s = \Omega_{s0}(1 + z^2/L_z^2)$ for the local cyclotron frequency of the resonant species. The location of the resonance for this case is shown in Fig. 3. We assume that the density is constant over this region, so the number of resonant

The polarization of the wave resonant with minority species s in majority species i may be determined by,²⁹

$$\frac{E^+}{E_{\theta}} = -i \frac{4(X-1) + 2Y(X^2-1) - 4V}{4 - Y(X^2-1)(1+2i\eta) + 4V}, \quad (32)$$

where $X = \Omega_s/\Omega_i$, $Y = n_s m_s/n_i m_i$, and

$$V = \frac{k_{\parallel}^2 c^2}{\omega_{pi}^2} \cdot \frac{X^2 - 1}{X^2}; \quad \eta = \frac{\Omega_s}{|k_{\parallel}| v_{ts}} \sqrt{\frac{\pi}{2}}. \quad (33)$$

We can then determine E_{θ} in the rotating frame from Faraday's law assuming $E_z = 0$, $E_{\theta} = -(\tilde{\omega}/ck_{\parallel})B_r$.

As a numerical example, we consider minority heating of deuterium in the Maryland Centrifugal Experiment (MCX).²⁷ It was found that this device can reach $M_A \approx 1$, so we expect the contained modes to be resonant with a stationary ripple.³⁰ MCX can operate at $B = 0.2$ T, $n = 5 \times 10^{14}$ cm⁻³, $T_i = 40$ eV, and $\Omega_0 = 10^6$ s⁻¹. The device radius is 25 cm, the plasma width at the midplane is 20 cm, and the scale length in the parallel direction near the midplane is about 50 cm. If the plasma is mixed at

95% hydrogen and 5% deuterium, a 20 Gauss ripple with $m = -10$ and $k_{\parallel} = 0.1$ cm will produce 9 MW of power dissipation. In the rest frame, the power dissipation can be seen as an effective decrease in the plasma resistance (the power dissipated for fixed voltage is V^2/R).

The way the plasma responds to this heating will depend on the overall circuit the plasma is a part of. In MCX, the plasma is in series with a ballast resistor that has several times the plasma resistance, and the total voltage is kept constant.³¹ Because of this, as the plasma resistance decreases most of the power dissipation will be in the ballast resistor, and the efficiency of heating is reduced.

There are several methods one might use to determine the effectiveness of plasma heating. First, one can measure the total power dissipated in the circuit by knowing the voltage-current characteristic of the discharge. This can be compared with the above estimate for the dissipated power. Second, the reduced plasma resistance can be measured by comparing the plasma voltage with the total applied voltage. This value can be confirmed by measuring the Doppler shift of He II emission lines, which can be used to determine the $E \times B$ drift velocity.³¹ Finally, the heating will lead to an elevated Helium temperature, which can be measured by the Doppler broadening of He II emission lines.

A direct measurement of heating by this method would produce two important results for the theory described here. First, it would provide a validation of the theory of using stationary waves to drive rotation in rotating plasmas. Second, finding the magnitude of the diffusion coefficient could confirm the existence of contained modes in plasmas with sheared rotation. This could improve the efficiency of alpha channeling and plasma heating by reducing the magnitude of the required magnetic ripple. There would also be expanded opportunities for rotating plasma experiments, with the ability to control the plasma temperature and rotation profile.

VI. DISCUSSION/CONCLUSION

For alpha channeling as well as for cyclotron heating, it is important to exceed a threshold wave amplitude throughout the plasma region. For alpha channeling, there must be a large enough wave amplitude to remove the alpha particles within a slowing down time. For cyclotron heating, the power absorbed is also proportional to the wave amplitude. Achieving sufficient amplitude throughout the plasma is difficult because of the high mode numbers required. A wave with mode number m decays like $r^{|m|}$ in a vacuum, although the decay is reduced in the presence of a plasma.

The contained modes described here can play an important role in maintaining the wave amplitude across the plasma width. The modes are localized near the peak rotation speed, which is optimal for interacting with alpha particles and plasma heating. Increasing the wave

amplitude at and near the core could improve the efficiency of alpha channeling. For example, in simulations of alpha channeling around 30% of the alpha particles were removed by waves, while almost 40% remained in the device after the simulation.¹⁰ If the remaining particles could interact with the waves and exit, we expect an additional 2 MeV per particle could be converted to potential energy. This could result in a significant increase in recovered power, allowing the plasma to sustain itself at a lower fusion reaction rate or with a higher energy loss rate.

An advantage to these stationary waves is that they require very little power input to be maintained. In the rest frame, the wave is simply a magnetic ripple, and could be produced by permanent magnets or by superconducting magnets to minimize power consumption. For ion cyclotron heating, this means the coupling efficiency between the antenna and plasma does not reduce the heating efficiency. The energy for ion cyclotron heating is just ohmic heating produced by the increase in plasma current, due to the decrease in plasma resistance.

A number of further calculations are necessary to produce these contained modes in experimental plasmas. The axial profile due to the mirror field has not been determined here, nor has the mode amplitude been given as a function of the ripple magnitude. In practice it may be difficult to diagnose these modes, because they do not produce an external magnetic field. Still, the results here suggest that these contained modes exist over a broad range of parameters, and suitable plasmas for exciting the modes have been produced experimentally.^{27,30}

The concept of producing plasma rotation using waves is promising, and the contained eigenmodes described here could improve the effectiveness of this interaction. Using waves to drive rotation in plasmas may make centrifugal mirrors a viable fusion concept by eliminating the electrodes and endplates which cause the Alfvén CIV limitation. In addition, the power for the rotation does not need to be supplied externally, but is transferred directly from the charged fusion product. The result is a fusion reactor that is efficient and simple, requiring only circular mirror coils and small magnetic ripple fields for continuous operation.

ACKNOWLEDGEMENTS

This work was supported by the DOE under Contract Nos. DE-FG02-06ER54851 and DE-AC0276-CH03073.

Appendix A: Derivation of effective potential

When we solve Eq. (6) for B_{1r} and $B_{1\theta}$, we find,

$$B_{1r} = ik_{\parallel}\Lambda \left[c_1 \frac{m}{r} B_{1z} - c_2 \frac{\partial B_{1z}}{\partial r} \right] \quad (\text{A1})$$

$$B_{1\theta} = k_{\parallel}\Lambda \left[(c_2 - c_3) \frac{m}{r} B_{1z} - (c_1 + c_4) \frac{\partial B_{1z}}{\partial r} \right] \quad (\text{A2})$$

where,

$$\Lambda^{-1} = \left(\frac{\tilde{\omega}^2}{v_A^2} - k_{\parallel}^2 \right)^2 - k_{\parallel}^4 \left(\frac{\tilde{\omega}^2}{\Omega_i^2} - \frac{\Omega' r}{\Omega_i} \right) - k_{\parallel}^2 \frac{v'_{0\theta}}{\Omega_i} \frac{\tilde{\omega}^2}{v_A^2}$$

$$c_1 = \frac{\tilde{\omega}^2}{v_A^2} \frac{\tilde{\omega}}{\Omega_i},$$

$$c_2 = k_{\parallel}^2 + k_{\parallel}^2 \frac{\Omega' r}{\Omega_i} - \frac{\tilde{\omega}^2}{v_A^2} - k_{\parallel}^2 \frac{\tilde{\omega}^2}{\Omega_i^2},$$

and,

$$c_3 = \frac{\tilde{\omega}^2}{v_A^2} \frac{v'_{0\theta}}{\Omega_i}; \quad c_4 = \frac{\Omega \tilde{\omega}}{v_A^2}.$$

We can then determine the equation for B_{1z} by using Eq. (A1) and (A2) together with $\nabla \cdot \mathbf{B} = 0$, leading to,

$$0 = \frac{\partial^2 B_{1z}}{\partial r^2} + \left(\frac{1}{r} + \frac{c'_2}{c_2} + \frac{\Lambda'}{\Lambda} + \frac{c_4 m}{c_2 r} \right) \frac{\partial B_{1z}}{\partial r} - \left(\frac{m^2}{r^2} - \frac{c_3 m^2}{c_2 r^2} + \frac{m}{r} \frac{\Lambda^{-1}}{c_2} \frac{\partial (c_1 \Lambda)}{\partial r} + \frac{\Lambda^{-1}}{c_2} \right) B_{1z} \quad (\text{A3})$$

We can now define,

$$f(r) = \frac{1}{2} \left(\frac{1}{r} + \frac{c'_2}{c_2} + \frac{\Lambda'}{\Lambda} + \frac{c_4 m}{c_2 r} \right) \quad (\text{A4})$$

and transform to $b = B_{1z} e^{\int_{r_0}^r f dr}$, to find,

$$\frac{d^2 b}{dr^2} - V_{\text{eff}}(r, \omega) b = 0, \quad (\text{A5})$$

with,

$$V_{\text{eff}} = \left(1 - \frac{c_3}{c_2} \right) \frac{m^2}{r^2} + \frac{m}{r} \frac{\Lambda^{-1}}{c_2} \frac{\partial (c_1 \Lambda)}{\partial r} + \frac{\Lambda^{-1}}{c_2} + f^2 + f'. \quad (\text{A6})$$

- ¹B. Lehnert, Nuclear Fusion **11**, 485 (1971).
²D. D. Ryutov, Soviet physics, Uspekhi **31**, 300 (Jan 1988).
³B. Lehnert, Physica Scripta **9**, 189 (Mar 1974).
⁴A. A. Bekhtenev, V. I. Volosov, V. E. Pal'chikov, M. S. Pekker, and Y. N. Yudin, Nuclear Fusion **20**, 579 (1980).
⁵V. Volosov, Nuclear Fusion **46**, 820 (Aug 2006).
⁶H. Alfvén, Rev. Mod. Phys. **32**, 710 (Oct 1960).
⁷B. Lehnert, J. Bergstrom, and S. Holmberg, Nuclear Fusion **6**, 231 (1966).
⁸A. J. Fetterman and N. J. Fisch, Phys Rev Lett **101**, 205003 (Nov 2008).
⁹A. J. Fetterman and N. J. Fisch, Plasma Sources Science and Technology **18**, 045003 (Nov 2009).
¹⁰A. J. Fetterman and N. J. Fisch, Phys Plasmas **17**, 042112 (2010).
¹¹A. J. Fetterman and N. J. Fisch, Fusion Sci Technol **57**, 343 (2010).
¹²N. J. Fisch and J. M. Rax, Phys Rev Lett **69**, 612 (Jan 1992).
¹³N. J. Fisch, Phys Rev Lett **97**, 225001 (2006).
¹⁴N. J. Fisch, Phys Plasmas **2**, 2375 (1995).
¹⁵A. I. Zhmoginov and N. J. Fisch, Phys Plasmas **15**, 042506 (Jan 2008).
¹⁶B. Coppi, G. Penn, and C. Riconda, Annals of Physics **261**, 117 (Jan 1997).
¹⁷E. J. Valeo and N. J. Fisch, Phys. Rev. Lett. **73**, 3536 (Dec 1994).
¹⁸N. J. Fisch and M. C. Herrmann, Nucl **35**, 1753 (1995).
¹⁹N. J. Fisch and M. C. Herrmann, Plasma Phys. Control. Fusion **41**, A221 (1999).
²⁰M. C. Herrmann, *Cooling alpha particles with waves*, Ph.D. thesis, Princeton University, Princeton, NJ (1998).
²¹D. Clark and N. Fisch, Phys Plasmas **7**, 2923 (Jan 2000).
²²N. Gorelenkov, N. Fisch, and E. Fredrickson, Plasma Phys Contr F **52**, 055014 (May 2010).
²³Y.-M. Huang and A. B. Hassam, Phys Rev Lett **87**, 235002 (Nov 2001).
²⁴T. Cho, M. Yoshida, J. Kohagura, M. Hirata, T. Numakura, H. Higaki, H. Hojo, M. Ichimura, K. Ishii, K. Islam, A. Itakura, I. Katanuma, Y. Nakashima, T. Saito, Y. Tatematsu, M. Yoshikawa, Y. Kojima, S. Tokioka, N. Yokoyama, Y. Tomii, T. Imai, V. Pastukhov, and S. Miyoshi, Phys Rev Lett **94**, 085002 (Jan 2005).
²⁵V. I. Volosov, Plasma Phys. Rep. **35**, 719 (Sep 2009).
²⁶G. F. Abdrashitov, A. V. Beloborodov, V. I. Volosov, V. I. Kubarev, Y. S. Popov, and Y. N. Yudin, Nuclear Fusion **31**, 1275 (1991).
²⁷R. F. Ellis, A. Case, R. Elton, J. Ghosh, H. Griem, A. B. Hassam, R. A. Lunsford, S. J. Messer, and C. Teodorescu, Physics of Plasmas **12**, 55704 (2005).
²⁸T. H. Stix, Nuclear Fusion **15**, 737 (1975).
²⁹T. H. Stix, *Waves in plasmas* (American Institute of Physics, New York, 1992).
³⁰C. Teodorescu, R. Clary, R. F. Ellis, A. B. Hassam, R. A. Lunsford, I. Uzun-Kaymak, and W. C. Young, Phys Plasmas **15**, 042504 (Jan 2008).
³¹C. Teodorescu, R. Clary, R. F. Ellis, A. B. Hassam, C. A. Romero-Talamas, and W. C. Young, Phys Plasmas **17**, 052503 (Jan 2010).

The Princeton Plasma Physics Laboratory is operated
by Princeton University under contract
with the U.S. Department of Energy.

Information Services
Princeton Plasma Physics Laboratory
P.O. Box 451
Princeton, NJ 08543

Phone: 609-243-2245
Fax: 609-243-2751
e-mail: pppl_info@pppl.gov
Internet Address: <http://www.pppl.gov>